

Building Terrestrial Planets:

Why results of perfect-merging simulations are not quantitatively reliable approximations to accurate modeling of terrestrial planet formation

Nader Haghighipour^{1,2,3} and Thomas I. Maindl^{4,5}

nader@psi.edu

Abstract

Although it is accepted that perfect-merging is not a realistic outcome of collisions, some researchers state that perfect-merging simulations can still be considered as quantitatively reliable representations of the final stage of terrestrial planet formation. Citing the work of Kokubo & Genda [ApJL, 714L, 21], they argue that the differences between the final planets in simulations with perfect-merging and those where collisions are resolved accurately are small, and it is, therefore, justified to use perfect-merging results as an acceptable approximation to realistic simulations. In this paper, we show that this argument does not stand. We demonstrate that when the mass lost during collisions is taken into account, the final masses of the planets will be so different from those obtained from perfect-merging that the latter cannot be used as a valid approximation. We carried out a large number of SPH simulations of embryo-embryo collisions and determined the amount of the mass and water lost in each impact. We applied the results to collisions in a typical perfect-merging simulation and showed that even when the mass-loss in each collision is as small as 10%, perfect-merging can, on average, overestimate the masses of the final planets by $\sim 35\%$ and their water-contents by more than 18%. Our analysis demonstrates that, while perfect-merging simulations are still a powerful tool in proving concepts, they cannot be used to make predictions, draw quantitative conclusions (especially about the past history of a planetary system) and serve as a valid approximation to, or in lieu of the simulations in which collisions are resolved accurately.

¹Planetary Science Institute, Tucson, AZ, USA

²Institute for Astronomy, University of Hawaii-Manoa, Honolulu, HI, USA

³Institute for Advanced Planetary Astrophysics, Honolulu, HI, USA

⁴SDB Science-driven Business Ltd, Larnaca, Cyprus

⁵Department of Astrophysics, University of Vienna, Vienna, Austria

Subject headings: Planet formation(1241), Solar system formation(1530), N-body simulations(1083)

1. Introduction

The classical model of terrestrial planet formation has had significant contributions to our understanding of the formation of Earth and the origin of its water. This model that uses N-body integrations to simulate the collisions and orbital evolution of gravitationally interacting bodies has demonstrated that terrestrial planets form through giant impacts among planetary embryos (e.g., [Kokubo & Ida 1998](#); [Chambers & Wetherill 1998, 2001](#); [Agnor et al. 1999](#); [Chambers 2001](#); [Kokubo et al. 2006](#)), proved that Earth’s water was brought to its accretion zone by hydrated protoplanetary bodies from the outer regions of the asteroid belt (e.g., [Morbidelli et al. 2000](#); [O’Brien et al. 2014, 2018](#); [Haghighipour & Winter 2016](#)), and presented models to account for the small mass of Mars ([Walsh et al. 2011](#); [Izidoro et al. 2014](#); [Clement et al. 2019a](#); [Nesvorny et al. 2021](#)) and even a possible origin for Mercury ([Clement et al. 2019b, 2021a,b](#); [Clement & Chambers 2021](#)).

As successful as it has been, the classical model and its N-body integrations suffer from an important shortcoming: they consider collisions to be perfectly inelastic. That means, when two objects collide, the colliding bodies are completely merged and no breakage, fragmentation, and debris is considered. This perfect-merging recipe also assumes that during a collision, the internal compositions (e.g., water-contents) of the colliding bodies stay intact and when collided, the entire composition of each object is transferred to the merged body. As a result, planets that are produced in the classical simulations carry more mass and water than they would have if simulations had included fragmentation, and had the transfer of water been treated properly. As the overestimation of mass directly affects the dynamical evolution and orbital architecture of the final planets, when combined with the overabundance of water, it indicates that planets produced by the classical model cannot be considered as reliable representations of observational and geological data. In other words, the classical model cannot be quantitative and cannot make predictions.

In reality, collisions are not perfectly inelastic. They produce fragments and large amounts of debris. A realistic model of terrestrial planet formation needs to take this into account. In the past decade, several groups have addressed this issue by resolving collisions using high-resolution simulations (e.g., [Marcus et al. 2009, 2010](#); [Kokubo & Genda 2010](#); [Stewart & Leinhardt 2012](#); [Leinhardt & Stewart 2012](#); [Chambers 2013](#); [Maindl et al. 2013, 2014](#); [Carter et al. 2015, 2018](#); [Bonsor et al. 2015](#); [Wallace et al. 2017](#); [Burger et al. 2018, 2020](#)). However, despite its fundamental shortcomings, the classical model and

its perfect-merging approach have stayed deeply popular. This popularity, that is mainly because of the ease of computations, is primarily based on the results of the fundamental works of Kokubo & Genda (2010) and Genda et al. (2012). These authors carried out a large number of Smooth Particle Hydrodynamics (SPH) simulations of the collisions of planetary embryos and, following the seminal work of Agnor & Asphaug (2004), identified an empirical value for the impact velocity that they used as the criteria to determine the outcome of embryo-embryo collisions. Kokubo & Genda (2010) showed that for the values of the impact velocity above this threshold, the two colliding bodies may break, shatter, or undergo a hit-and-run event (similar results had also been obtained by Asphaug 2009). However, for lower values, collisions may produce one large body along with debris and possibly even small fragments. These authors argued that because during the formation of (terrestrial) planets, it is the large body that has the most contribution, it is justified to ignore the debris and few fragments, and consider/define such events as accretion (or merging). Kokubo & Genda (2010) showed that in their SPH simulations to which their above definition of accretion applies, the final mass and number of terrestrial planets were similar to those obtained from N-body integrations with perfect-merging. The supporters of the perfect-merging scenario argue that, although the accretion events by Kokubo & Genda (2010) are not 100%, the difference between their outcomes and those of perfect-merging simulations is not large enough, and results of perfect-merging simulations can be used as a valid and reliable approximation to simulations where collisions are resolved accurately.

Although the conclusions drawn by Kokubo & Genda (2010) and Genda et al. (2012) are valid within the context of their simulations, when used as the basis for the argument that the error in using perfect-merging recipe is negligible, do not provide a solid ground. The reason lies in the fact that when labeling a collision as accretion, the amount of the mass that did not contribute to the formation of the single body (e.g., debris) was ignored. Kokubo & Genda (2010) and Genda et al. (2012) argued that because their focus was on modeling the formation of terrestrial planets, only collisions that produced a single body were the most relevant ones, and for that reason, they categorized collisions into only two categories of hit-and-run (non-merging) and non-hit-and-run (merging) events. As a result, many cases in which debris and/or some fragments were produced and scattered out of the accretion zone were labeled as accretion events without their mass-losses being taken into account. (We would like to note that in a later study Genda et al. 2015, returned to their previous N-body simulations and calculated the debris produced in each system. We will discuss their results in more detail in sections 3.4).

While it is possible that in systems where the final planet forms after only one or two collisions, the total mass-loss may be small, when considered in the larger context of planet formation, where embryos are subject to many collisions, the cumulative loss of

mass (and volatiles such as water) may not be negligible. The purpose of this paper is to demonstrate the latter. We have carried out a large number of SPH simulations of embryo-embryo collisions and calculated the amount of the mass and water lost in each case. We have also carried out a suite of simulations of terrestrial planet formation using the classical model, and determined the mass and water-contents of their final planets using the perfect-merging approach. We will show that when the mass-loss obtained from SPH simulations is applied to the simulations of classical model, the cumulative loss of mass and water during the formation of a planet will be so large that the final outcome of the perfect-merging scenario will be quantitatively unreliable.

The outline of this paper is as follows. In the next section, we will explain the details of our methodology and approach. In Section 3, we analyze the results and compare them with previous studies. In Section 4, we discuss the implications of our findings and present our concluding remarks.

2. Numerical Simulations

2.1. Perfect-Merging (Classical Model)

We began by carrying out perfect-merging simulations in the context of the classical model. Each simulation started with a disk of protoplanetary bodies extending from 0.5 AU to 4 AU. The disk consisted of 1000-1200 planetesimals and 76 planetary embryos. The bimodality of the disk was to include dynamical friction (e.g., [Ida & Makino 1992](#); [O’Brien et al. 2006](#); [Morishima et al. 2008](#)) and to ensure that the starting systems would be consistent with the outcomes of Runaway and Oligarchic growths ([Kokubo & Ida 1998](#); [Kokubo et al. 2000](#); [Darriba & Haghighipour 2021](#)). The embryos were distributed according to the surface density $10 \text{ (g cm}^{-2}\text{)} (r/\text{AU})^{-\alpha}$, $\alpha = 0.5, 1, 1.5$, and planetesimals were distributed uniformly. The masses of embryos, ranging between 0.015 and 0.071 Earth-masses, were scaled with their distances to the Sun (r) and the number of their mutual Hill radii (Δ) as $r^{3(2-\alpha)/2} \Delta^{3/2}$ ([Kokubo et al. 2000](#); [Raymond et al 2005a,b, 2009](#); [Izidoro et al. 2013, 2014](#); [Haghighipour & Winter 2016](#)). The distances between planetary embryos were randomly chosen to vary between 5 and 10 mutual Hill radii.

We considered every planetesimal to have an initial mass of 20% lunar-mass. As explained in section 3.2, we did not treat planetesimals as test particles and included their masses when calculating the final mass of a planet. We assigned water to all bodies according to the following: Bodies interior to 2 AU were considered to have a water-mass fraction of 10^{-5} , those between 2 AU and 2.5 AU to have 0.1% water in mass and those beyond 2.5

AU to have a water-mass fraction of 10%. We also assumed that no earlier radial mixing had smoothed out the water distribution in the protoplanetary disk (e.g., [Carter et al. 2015](#)).

Simulations were carried out both with and without giant planets. When including giant planets, two cases of Jupiter-only and Jupiter-Saturn were considered. We placed these planets in their current semimajor axes and carried out simulations for the values of their eccentricities equal to 0, 0.1, and their current values.

In total, we carried out 42 simulations. We integrated each system for 200 Myr using the hybrid routine in the N-Body integration package MERCURY ([Chambers 1999](#)). The time-step of integrations were set to 6 days. In general, in each simulation, 1 to 4 planets formed interior to 2.1 AU with most simulations forming 3 planets. A typical simulation produced 45 to 60 embryo-embryo collisions (giant impacts) and 200 to 320 embryo-planetesimal collisions. The number of giant impacts that resulted in the formation of a planet varied between 6 and 11. Collisions among planetesimals were not included.

Figure 1 shows a sample of our results. In this simulation $\alpha = 1.5$, Jupiter and Saturn are in their current orbits and carry their current eccentricities. The protoplanetary disk in this simulation has a total mass of ~ 5 Earth-masses with a planetesimal to embryo mass-ratio of ~ 1 . The color-coding demonstrates the water-mass fraction (WMF) of each object. We will use this simulation and its final results (shown by the panel at 200 Myr) to demonstrate the errors in using perfect merging as a quantitative model. We would like to note that the differences between the orbital assembly as well as the physical and compositional properties of the final planets in figure 1 and those of the terrestrial planets in our solar system are expected results that have roots in the fact that all simulations of planet formation are stochastic and their results must be studied statistically.

2.2. SPH Simulations of Embryo-Embryo Collisions

To determine the amount of mass and volatiles (specifically water) lost during an impact, we carried out a large number of SPH simulations of embryo-embryo collisions using our 3D, solid-body, continuum-mechanics SPH code MILUPHCUDA ([Maindl et al. 2013](#); [Schäfer et al. 2016, 2020](#)). Our code solves the continuity equation and the equation of the conservation of momentum in continuum mechanics, and includes self-gravity. We discretized the solid body continuum into mass packages (i.e., SPH particles) and used the locations of these particles as the sampling points of the numerical method. The SPH particles move similar to point masses following the equation of motion. Each particle carries all physical properties of the part of the solid body that it represents (e.g., mass, momentum, and energy). To

simulate the plastic behavior of solid materials, we followed [Collins et al. \(2004\)](#) and [Jutzi \(2015\)](#), and used pressure-dependent strength models. Fractures and brittle failures were handled by implementing the Grady-Kipp fragmentation model ([Grady & Kipp 1980](#); [Benz & Asphaug 1995](#)). We ensured first-order consistency by applying a tensorial correction as presented by [Schäfer et al. \(2007, 2016\)](#). Dissipation of kinetic energy into heat was modeled by tracking inner energy including viscous energy terms originating from artificial viscosity ([Monaghan & Gingold 1983](#)).

We considered embryos to be silicate rocks composed of pure basalt or basalt and water. Basaltic rock is commonly used as the material of rocky bodies from centimeter-sized grains to the mantles of large asteroids such as Ceres ([Melosh & Ryan 1997](#); [Agnor & Asphaug 2004](#); [Michel 2009](#); [Nakamura & Michel 2009](#)). We used the Tillotson equation of state ([Tillotson 1962](#); [Melosh 1996](#)) to model the materials of the colliding bodies. The parameters for basalt and water-ice were taken from [Melosh \(1996\)](#) and [Benz & Asphaug \(1999\)](#) and are given in Table 1. We also implemented a damage model using Weibull distribution of strain level ϵ given by $n(\epsilon) = k\epsilon^m$ ([Weibull 1939](#)). We used the Weibull parameters $(m, k) = (16, 10^{61} \text{ m}^{-3})$ for basalt ([Nakamura et al. 2007](#)) and $(9.1, 10^{46} \text{ m}^{-3})$ for ice ([Lange et al. 1984](#)), respectively.

Figure 2 shows the geometry of an impact. We considered the target to be at rest and allowed the impactor to collide with it while moving with the impact velocity v_{imp} given in the units of mutual escape velocity $v_{\text{esc}}^2 = 2G(m_t + m_i)/(R_t + R_i)$. Here, m_t and m_i are the masses of the target and impactor, and R_t and R_i represent their corresponding radii, respectively. The impact angle was chosen such that $\alpha = 0$ would be a head-on collision and $\alpha = 90^\circ$ would represent a grazing impact. We chose the impactor to be 100% basaltic rock and the target to be a silicate rock composed of basalt with 30% water in its mantle and crust. When modeling collisions, we considered water to be surface ice on the top of a solid layer (a water shell on the top of the mantle).

Figure 3 shows a sample of the results. Here we show the amount of water lost in an impact between two Ceres-sized bodies for different values of their impact angle and impact velocity. The color-coding represents water-loss per collision in terms of the total mass of the colliding bodies [wt-% short for weight-percent, representing mass-fraction]. We define water-loss as the fraction of total water that is no longer gravitationally bound to the “surviving bodies” (i.e., the outcome of an impact). For a given material strength, the surviving bodies depend on the impact velocity and angle. In the simulations of figure 3, three types of outcome were obtained: merging, where one major body was produced along with debris that was lost; hit-and-run, where two major bodies survived along with debris that was lost; and erosion, where we considered only the two largest fragments as surviving

bodies (for a quantitative definition of these outcomes, we refer the reader to [Leinhardt & Stewart 2012](#)). We would like to emphasize that the collision outcome “merging” does not refer to “perfect merging” in which the two colliding bodies undergo perfectly inelastic collision and are completely merged. Unlike in the perfect-merging scenario, a merging event produces debris that in most cases is lost to space.

Because we are interested in both the loss of mass and water, we chose to show the amount of water-loss as it can also be used as a proxy for mass-loss. As shown here, the loss of water (and mass) varies from very small values close to 10% (in agreement with the results of [Kokubo & Genda 2010](#)) to more than 90%. For example, 42 % of our collisions resulted in merging with an average water-loss of 7 wt-% (population variance = 1 wt-%), 33 % resulted in hit-and-run with an average water-loss of 5 wt-% (population variance = 0.2 wt-%), and 25 % resulted in erosion with an average water-loss of 74 wt-% (population variance = 4 wt-%). Figure 3 also shows that the loss is small for low impact velocities irrespective of the impact angle, and for collisions close to grazing impacts.

It is important to note that the overall average of water-loss in all our simulations is ~ 23 wt-%. However, this value has no physical meaning because the initial values of impact angles and velocities in our simulations had not been chosen to resemble their distribution in a typical planet formation scenario. They had been selected to cover a large region of the parameter-space. In the next section, we use results shown in figure 3 to calculate the total loss in mass and water for the final planets of figure 1.

3. Results and Analysis

3.1. Calculation of Mass- and Water-Loss

In this section, we will demonstrate that when the results of the SPH simulations of section 2.2 are applied to the perfect-merging planets of section 2.1, the cumulative loss of mass and water will not be negligible.

We start by using a simple system and some simple assumptions to portray the general picture of the concept that we are trying to show (i.e., the significance of mass-loss in multiple collisions). Let’s assume, for the mere sake of argument, that the definition of accretion as stated by [Kokubo & Genda \(2010\)](#) and [Genda et al. \(2012\)](#) stands. That is, if two embryos collide, regardless of how much debris and fragments are produce, as long as one main body is formed, that event is labeled accretion (or merging). Also, merely for the purpose of demonstration, let’s assume that in any embryo-embryo collision, a fixed fraction η of the total colliding masses is lost after collision. That is, if an embryo with a mass m_1 impacts an

embryo with a mass m , irrespective of their material strength and their angle and velocity of impact, the post-impact mass of the merged body will be $(1 - \eta)(m + m_1)$ indicating that $\eta(m + m_1)$ amount of mass was lost due to the collision. This assumption is not fully realistic because the mass of the collisional debris varies based on the mass, material strength, and dynamical properties of the colliding bodies. However, for the purpose of demonstrating the concept, it is useful.

Let's now assume that the first merged body with the mass $(1 - \eta)(m + m_1)$ is impacted by an embryo with a mass m_2 . According to our assumption, the amount of mass lost during this impact will be $\eta[(1 - \eta)(m + m_1) + m_2]$ and the new merged body will have a total mass of $(1 - \eta)[(1 - \eta)(m + m_1) + m_2]$. Continuing in the same fashion, the total amount of mass lost after n impacts will be equal to

$$\text{Total Mass Loss} = \sum_{j=1}^n \eta(1 - \eta)^{n-j} m + \sum_{j=1, \dots, k}^n \eta(1 - \eta)^{n-k} m_k \quad k = 1, 2, \dots, n. \quad (1)$$

In this equation, m_k is the mass of the embryo that generates the k -th impact. It is important to note that the summation over j in the second term is carried out for each value of k , separately.

A closer look at the summation terms in equation (1) indicates that these terms are in fact geometric series and can be calculated analytically. For instance, the first summation, corresponding to the contribution of embryo m to the total mass-loss, is given by

$$\sum_{j=1}^n \eta(1 - \eta)^{n-j} m = [1 - (1 - \eta)^n] m. \quad (2)$$

Figure 4 shows the quantity $[1 - (1 - \eta)^n]$, the fraction of the mass of the first target (m) that is lost after n collisions. To be conservative, we show this quantity for three small values of $\eta = 5\%, 10\%, 15\%$. As shown here, although the amount of the mass lost in one impact is small, after only a few impacts, the total contribution of the first term of equation (1) becomes so large that it cannot be ignored (recall that in our perfect-merging simulations, the total number of embryo-embryo collisions that resulted in the formation of a planet was between 6 and 11). Applying similar analysis to other terms of equation (1), combined with the fact that planetary embryos, in addition to colliding with other embryos, are also impacted by planetesimals will clearly demonstrate that the error in ignoring mass-loss in the course of the formation of a planet is not negligible. In the following, we demonstrate

the latter for the final planets of figure 1 by directly calculating the amount of mass that is lost in each collision during their formation.

3.2. Mass-loss in Figure 1

To determine the amount of the mass that is lost during the accretion of the final three planets of figure 1, it is necessary to identify the seed embryo for each planet. Because in a perfect-merging collision, the entire mass of the impactor is accreted by the target, it is possible to identify the seed object by tracking back through collisions. Table 2 shows this for the final planets of figure 1. To identify the planets, we have labeled them by numbers 1, 2 and 3 corresponding to the planet on the left, middle and right in the last panel of figure 1, respectively. We have also given their final semimajor axes to further ensure their identification.

Table 2 also shows the initial mass and water content of each seed embryo and the number of its collisions. As shown here, in addition to impacting by embryos (shown by the entry “Collisions with embryos”), each growing seed was also impacted by a large number of planetesimals (shown by “Collisions with planetesimals”). It is important to note that during the evolution of the system, some of the embryos that collided with a growing seed, themselves were impacted by other embryos and planetesimals. As a result, the final mass of a planet, and with the same token, the total mass of its collisional debris, are the results of a larger number of impacts. We have shown these quantities by “Total embryo-embryo collisions” and “Total embryo-planetesimal collisions” for each seed.

To calculate the final mass of a seed and the amount of the mass that was lost during its growth, we assumed that all embryo-planetesimal collisions were perfectly inelastic (produced no debris) and resulted in the complete accretion of the planetesimal. Therefore, after each collision of a planetesimal with an embryo, we added the mass of the planetesimal (20% lunar-mass) to the mass of that embryo.

To calculate the collisional debris produced in each embryo-embryo impact, we used the results shown in figure 3. As indicated by this figure, for a large portion of the parameter-space, the amount of the mass lost in each impact is at a level smaller than 20%. We, therefore, took a conservative approach and assumed that in all embryo-embryo collisions, 10% of the total colliding mass was lost in the form of debris or scattered fragments. We did not consider the re-accretion of the produced debris.

The entries “Total mass-loss” and “Final mass” in table 2 show the results. We would like to emphasize that these entries are only for their corresponding seed embryos and do

not indicate the mass-loss for the entire simulation. As expected, the total amount of mass that is lost in the formation of each of these planets is substantial, varying between 1.1 to almost 3.5 Mars-masses. These values are 53% to 71% smaller than their perfect-merging values and show $\sim 30\%$ to 45% error when the results of perfect-merging simulations are used as an approximation to realistic models.

3.3. Water-loss in Figure 1

The loss of water occurs when a hydrated embryo collides with a growing planet. Because not all embryos that are accreted by a planet carry water, the total amount of water that is lost during the formation of a planet will depend on the number of the hydrated embryos that collide with it, the time of their collision, and whether these embryos themselves had experienced impacts prior to being accreted by the planet. For instance, Planet-1 acquired its water when its seed embryo-8 had its last collision with a hydrated embryo from the region of 2-2.5 AU. Recall that embryos from that region carry 2% water. The hydrated embryo, itself, had been impacted by a dry embryo prior to its accretion by embryo-8 meaning that it had lost some of its 2% water before its last impact. The total loss of water in this case would then be equal to the sum of the water that is lost in the impact of the hydrated embryo with the dry embryo, and the amount of water that it lost in its subsequent collision with growing Planet-1.

Planet-2 acquired its water during its last two embryo-embryo impacts. At this stage, the planet accreted two hydrated embryos. The first embryo did not have any prior impacts. However, the second embryo had collided with a dry embryo before being accreted by the growing planet. In this case, the total amount of water-loss is equal to the water that is lost during the accretion of the first hydrated embryo, the amount of water that the second hydrated embryo lost in its collision with a dry embryo, and the water lost during the accretion of the second hydrated embryo. Planet-3 did not have any collision with a hydrated embryo,

Table 2 shows the fraction of the water that is lost in each of the two planets 1 and 2. To maintain focus on demonstrating the significance of water-loss and the error in neglecting this quantity, we assumed that during a collision, the only material that is lost would be water. That is, when a hydrated embryo undergoes a collision, the amount of its water decreases, however, the amount of its rock will stay intact. As a result, all non-hydrated embryos will maintain their full masses during a collision, and the only loss will be in the water of hydrated embryos. We also assumed that in any collision that involved hydrated embryos, 10% of the total water was lost and would never be re-accreted.

The entry “Final WMF” in table 2 presents the total water-content of the final planets after all water-losses have been taken into account. In calculating this quantity, we considered no loss of water in embryo-planetesimal collisions, however, we added the mass of each planetesimal to the mass of the final collision outcome. The “Perfect-Merging WMF” assumes that no water was lost during a collision and the entire water content of a hydrated embryo was distributed over the full perfect-merging mass of the final body. As shown here, in forming Planet-1, where water was delivered during the very last accreting impact, there is 16% error in using the perfect-merging scenario. This value increases to over 18% for Planet-2 where water was delivered during the last two collisions. These results demonstrate that not only does perfect-merging overestimate the water-content of the final bodies, the error introduced into calculations, especially for objects with substantial amount of water is non-negligible.

3.4. Comparison with previous studies

In this section, we compare the production of the debris in our simulations with those of previous studies. Debris production during terrestrial planet formation has been studied by a few authors, albeit in different contexts. For instance, in their study of the diversity of the outcome of giant impacts, [Stewart & Leinhardt \(2012\)](#) investigated the effect of the collision model of [Leinhardt & Stewart \(2012\)](#) on the late stage of terrestrial planet formation by carrying out Monte Carlo simulations of the formation of a single planet. These authors stated that the mass of the debris produced in their single-planet formation simulations was on average $\sim 15\%$ of the mass of the final planet. Taking at face value and applying to the result of figure 1, this percentage suggests approximately 1.2 Mars-mass of debris for planets 1 and 2, and 0.5 Mars-mass of debris for planet 3, which are almost half the “Total mass-loss” shown in table 2. As we explain below, such a low amount of debris is unrealistic and has roots in the fact that they were obtained from Monte Carlo simulations rather than actual N-body integrations. Unlike the latter, the final results of Monte Carlo simulations are not the product of the natural evolution of the initial system, and do not include the mutual interactions of all bodies. Also, the extreme sensitivity of N-body simulations to the initial conditions, combined with the fact that their final results are also extremely sensitive to the type of the codes in which they have been written, the type of the compiler, and the internal round-off errors associated with the architecture of the computers on which they have been carried out does not allow for randomly selecting initial conditions from different simulations. While Monte Carlo results are informative, as [Stewart & Leinhardt \(2012\)](#) have also mentioned, they cannot replace the outcome of N-body simulations. With the same token, these results cannot be generalized to all planet formation models as well.

A realistic study of debris production requires calculating the debris for each impact, using the mass and orbital elements of the colliding bodies at the moment of collision, while the N-body simulation is in progress. [Genda et al. \(2015\)](#) carried out somewhat similar simulations. They used the results of the SPH simulations of giant impacts by [Genda et al. \(2012\)](#) and determined the total mass of collisional fragments during embryo-embryo collisions in the N-body simulations of [Kokubo & Genda \(2010\)](#). Among many of their findings, these authors reported that an average of 4.2 Mars-masses (corresponding to $\sim 18\%$ of the initial mass of each system) turned into fragments in all their 50 N-body simulations. They also found that on average, in each impact, an equivalent of 0.2 Mars-mass was converted into debris.

[Genda et al. \(2015\)](#) stated that their 18% value is consistent with the 15% debris production reported by [Stewart & Leinhardt \(2012\)](#). However, as we explain below, this comparison is not entirely valid. First, as mentioned earlier, due to their nature (i.e., obtained from Monte Carlo simulations), results by [Stewart & Leinhardt \(2012\)](#) are not generalizable and cannot be used in lieu of the results of N-body integrations. In fact, the 18% fragment mass reported by [Genda et al. \(2015\)](#) is more applicable to general N-body simulations than the results by [Stewart & Leinhardt \(2012\)](#). Second, it is important to note that the 15% value reported by [Stewart & Leinhardt \(2012\)](#) is 15% of the mass of the *final planet* whereas the 18% value reported by [Genda et al. \(2015\)](#) is 18% of the *initial mass* of the system (in all their N-body simulations, the initial mass was 2.3 Earth-masses). The two percentages have been obtained using different methods and cannot be compared.

Interestingly, if the 18% value reported by [Genda et al. \(2015\)](#) is applied to the simulation of figure 1 where the initial mass of the system is ~ 5 Earth-masses, the mass of the debris will be ~ 9 Mars-masses which is only slightly larger than the sum of all three values of “Total mass-loss” reported in table 2 ($2.52 + 3.46 + 1.10 = 7.08$ Mars-masses). Also, as reported by [Genda et al. \(2015\)](#), each of their giant impacts produced fragments with the total mass of 0.2 Mars-masses. Multiplying this value by the total number of embryo-embryo collisions in table 2, the amount of mass-loss will range between 1.8 to 3.6 Mars-masses, consistent with the total mass-loss found in our simulation.

It is, however, important to mention that the above 18% fragment-mass and 0.2 Mars-mass debris per impact must be taken with caution. The reason is that when calculating the debris in a giant impact, [Genda et al. \(2015\)](#) did not take into account the loss of mass in previous impacts of the same body. For instance, if an object X was impacted by a body A and later by another body B, the loss of mass on XA due to the X-A impact was not considered when the debris produced in XA-B impact was calculated (instead, the full perfect-merging mass of XA was used). In other words, and as also mentioned by [Genda et](#)

al. (2015), the above 18% fraction and 0.2 Mars-mass have been overestimated. It is for that reason that when these values are applied to the total number of embryo-embryo collisions in our simulations, they result in more mass-loss than reported in table 2. This suggests that even though all collisions do not produce the same amount of debris, our assumption of a fixed 10% mass-loss per giant impacts is conservative enough to validly demonstrate the point of our argument.

The most recent calculation of giant impact debris is that of Crespi et al. (2021). These authors used the outcomes of 880 SPH simulations of the collisions of protoplanetary bodies and calculated the mass of the debris in 1356 giant impacts obtained from 11 N-body simulations of the late stage of terrestrial planet formation. Crespi et al. (2021) reported that the least amount of the debris produced in each of their embryo-embryo impacts was approximately 0.42 percent of the total colliding masses. These authors acknowledged that this value is too conservative and that more realistically, 18% to 24% of the initial mass of a system may be converted into debris.

The above 18-24% range is obtained from the results of the current state-of-the-art simulations of terrestrial planet formation by Burger et al. (2020). As mentioned earlier, accurate calculations of collisional mass-loss requires determining the amount of the debris for each impact, at the moment that it occurs, and by including the post-collision bodies with their post-collision masses in the N-body integrations, without interrupting the process. Burger et al. (2020) carried out such simulations. These authors introduced, for the first time, a hybrid approach to N-body simulations in which each giant impact is resolved accurately with an SPH code and its results are inserted back into the N-body integrations while the latter is in progress. Burger et al. (2020) calculated the total amount of the collisional debris for each N-body simulation and showed that it varies between 1.1 and 1.5 Earth-masses (see the entry “ $M_{\text{col-losses}}$ ” in their table 2). These authors stated that the initial mass of each of their systems was 6.1 Earth-masses indicating that 18-24% of the initial material was lost as collisional debris. Applying this range of mass-loss to our simulations, where initially each system had ~ 5 Earth-masses of material, the total mass lost during the formation of the final system of figure 1 would be at least at the level of 9 Mars-masses which is slightly larger than the 7.08 Mars-masses reported in table 2. Once again, this agreement with previous results indicates that our 10% loss per impact is not far from reality, and the results reported here are reliable.

4. Discussion and Concluding Remarks

Motivated by the argument that the differences between the results of the perfect-merging simulations of terrestrial planet formation and those in which collisions are simulated more accurately are so small that perfect-merging results can be used as a quantitatively acceptable approximation to realistic models, we studied the effect of the loss of material during giant impacts on the mass and water content of the final planets to examine the validity of the above argument. We carried out an analytic study and showed that when the formation of a planet requires more than one or two giant impacts (which, most often is the case in actual N-body simulations), the cumulative loss of mass during collisions will be substantially large and cannot be ignored (figure 4).

To demonstrate the latter, we carried out a large number of SPH simulations of collisions between two Ceres-sized embryos and determined the amount of the mass and water that was lost in each collision. We applied these results to embryo-embryo collisions in a sample simulation of the classical model of terrestrial planet formation and showed that even when the amount of mass-loss in a single collision is small, the cumulative amount of the mass that is lost in all collisions that result in the formation of a planet are so large that if perfect-merging approach is used, considerable error will be introduced to the final results. We also showed that not only does perfect-merging highly overestimate the mass of the final planets (at times by several folds, see table 2), it also overestimates the water-contents of the final bodies giving the false impression that some of the terrestrial planets in our solar system might have carried a large amount of water in the past.

To maintain focus on demonstrating the significance of the mass and water losses during collisions, we made two simplifying assumptions. First we assumed that irrespective of the size, material composition, and impact parameters of an embryo, same percentage of the total mass or total water of colliding bodies would be lost in each embryo-embryo collision. This mass-loss can be in the form of debris, scattered fragments, and evaporated water. Because from our SPH simulations of the collisions of Ceres-sized bodies (figure 3), for a large range of the parameters, the amount of loss is at the level of 20%, we took a conservative approach and assumed that in each collision, 10% of the total mass or water is lost in the form of debris. As demonstrated in Section 3.2, these assumptions resulted in 1.10 to 3.46 Mars-masses of debris in the formation of each planet of figure 1 indicating large errors in using perfect-merging results as an approximation. A comparison with previous studies confirmed that although the assumption of a constant, fixed mass-loss per impact is not fully realistic, our 10% assumption is an appropriate approximation to reliably demonstrate the point of our argument, and the results produced with this assumption can be taken confidently.

That the cumulative collisional mass-loss during the formation of a planet is typically so

large that it does not allow perfect-merging to be a valid approximation to realistic models is based on the argument that if these mass-losses are taken into account (that is, N-body simulations are carried out while masses are removed after each impact), the final orbital elements and, therefore, the orbital architecture of the final planetary system will be so different from that of perfect-merging results that the latter cannot be considered as a viable approximation. We did not carry out such simulations (reducing the mass of colliding bodies by 10% and continuing the N-body integrations). However, such simulations have in fact been carried out by [Burger et al. \(2020\)](#). In their state-of-the-art approach to simulating terrestrial planet formation where giant impacts are resolved using SPH simulations (and without using a collisional catalog or scaling law) and are incorporated into the N-body integrations while the latter is in progress, these authors demonstrated that when collisional mass-losses are taken into account, the final planetary systems will be much different from those obtained from perfect-merging simulations (we refer the reader to figure 2 of [Burger et al. 2020](#)).

It is understood that in some collisions, the amount of the lost mass may be smaller than the above 10%. However, it is important to note that these smaller mass-losses may be complemented by the debris that are produced during embryo-planetesimal collisions. To avoid computational complications, we assumed that in these collisions, planetesimals would be fully accreted and no debris would be produced. However, given the mass of individual planetesimals (0.2 lunar-mass), it is inevitable, especially at the early stages of the growth when the seed embryos are still small, that some debris would in fact be generated. This debris too will contribute to the total mass- and water-loss. In connection to the values reported in table 2, this means that although the values of the final masses and water-contents of the planets may not be exact, when all sources of mass- and water-loss are taken into account, the ranges of error given by table 2 are reliable.

In calculating the final mass of a planet, we did not consider the re-accretion of the debris. Previous studies (e.g., [Benz et al. 2007](#); [Kobayashi & Tanaka 2010](#)) have shown that the time of the production and re-accretion of collisional debris may be comparable, suggesting that the process of re-accretion could be efficient. For instance, [Benz et al. \(2007\)](#) showed that in collisions that might have stripped the mantle of Mercury, 30% of the generated debris was re-accreted. However, the recent study of giant impacts by [Crespi et al. \(2021\)](#) indicates that most of the ejecta produced in giant impacts are closer to the central star than their points of impact, meaning that their re-accretion may not be as efficient as in the case of giant impacts with Mercury.

As shown by table 2, the errors in mass and water estimation increase by the number of collisions. While this is intuitive and an expected result, it is important to discuss its

implications especially in connection to the water-contents of the final bodies. We remind that in the simulation of figure 1, planets 1 and 2 received water through one and two impacts by hydrated embryos at the end of their formation. Some of those hydrated embryos had also been impacted by other embryos (and planetesimals) prior to their final accretion. Those number of collisions, although small, still introduced approximately 18% error in estimating the WMF of the final planetary bodies when the water-loss per impact was 10%. For a planet with a higher WMF, not only more hydrated embryos would be accreted, there is a high probability that those embryos would have more pre-accretion impacts as well. In other words, in a perfect-merging scenario, as the WMF of bodies increase, so does the overestimation of their water-content, and most likely with a higher rate than those with small number of impacts. That means, when modeling the formation of the terrestrial planets of our solar system, unless proper calculations are made to determine the actual WMF of planets in a perfect-merging simulation, any comparison of the final water-contents of planets in such models with the current values of the water-contents of terrestrial planets would be misleading and can result in drawing incorrect conclusions. For instance, they may give the wrong impression that some of the terrestrial planets in the solar system had more water in the past, falsely motivating scientists to develop models to explain how those planets lost their water.

In the sample perfect-merging simulation used in this study (figure 1), the number of big impacts received by each seed embryo is between 7 and 10. This number is consistent with our understanding of the dynamical evolution of the protoplanetary disk in the inner region of the solar system. For instance, Embryo-30, the seed for Planet-3, is close to the region of the influence of the ν_6 secular resonance (at ~ 1.8 AU) where most objects are scattered out of the system (we refer the reader to [Haghighipour & Winter 2016](#), for a complete discussion of the effect of secular resonances on terrestrial planet formation). As a result, this embryo receives the least number of impacts. In contrast, Embryos 8 and 28, being farther in and away from the ν_6 resonance, receive more collisions. We would like to note that although Embryos 8 and 28 are close to the location of ν_5 resonance at ~ 0.7 AU, as shown by [Haghighipour & Winter \(2016\)](#) and [Levison & Agnor \(2003\)](#), this resonance is not strong enough to have significant effects on the dynamics of planetary embryos in that region.

In closing, we would like to emphasize that, as demonstrated by its successful history, the classical model and the perfect-merging recipe are still the most powerful tools for proving concepts and exploring the physical processes that are involved in the late stage of terrestrial planet formation. However, for the purpose of explaining the dynamical and compositional properties of Earth and other terrestrial planets, and in order to be able to extend those models to other planetary systems, it is imperative that collisions be simulated accurately and

the effects of debris and fragments be taken into account (e.g., [Maindl et al. 2014](#); [Burger et al. 2020](#)). In that respect, perfect-merging cannot offer a scientifically viable approximation that can be used to draw quantitatively valid conclusions and make meaningful predictions.

NH would like to express his gratitude to the Information Technology division of the Institute for Astronomy at the University of Hawaii-Manoa for maintaining computational resources that were used for carrying out the numerical simulations of this study. We are thankful to the anonymous referee for their critically reading our manuscript and constructive recommendations. Our thanks also go to Christoph Burger for fruitful discussions. Support is acknowledged for NH through NASA grants 80NSSC18K0519 and 80NSSC21K1050, and NSF grant AST-2109285. TIM acknowledges support from Austrian Science Fund (FWF) project P33351-N.

REFERENCES

- Agnor, C. B., Canup, R. M. & Levison, H. F. 1999, *Icarus*, 142, 219
- Agnor, C. & Asphaug, E. 2004, *ApJL*, 613, L157
- Asphaug, E. 2009, *AREPS*, 37, 413
- Benz, W. & Asphaug, E. 1995, *Comput. Phys. Comm.*, 87, 253
- Benz, W. & Asphaug, E. 1999, *Icarus*, 142, 5
- Benz, W., Anic, A., Horner, J. & Whitby, J. A. 2007, *SSRv*, 132, 189
- Bonsor, A., Leinhardt, Z. M., Carter, P. J., Elliott, T., Walter, M. J. & Stewart, S. T. 2015, *Icarus*, 247, 291
- Burger, C., Maindl, T. I. & Schäfer, C. M. 2018, *CeMDA*, 130, 2
- Burger, C., Bázso, Á. & Schäfer, C. M. 2020, *A&A*, 634, id.A76
- Carter, P. J., Leinhardt, Z. M., Elliott, T., Walter, M. J. & Stewart, S. T. 2015, *ApJ*, 813, article id. 72
- Carter, P. J., Leinhardt, Z., M., Elliott, T., Stewart, S. T. & Walter, M. J. 2018, *E&PSL*, 484, 276
- Chambers, J. E. & Wetherill, G. W. 1998, *Icarus*, 136, 304

- Chambers, J. E. 1999, MNRAS, 304, 793
- Chambers, J. E. 2001, Icarus, 152, 205
- Chambers, J. E. & Wetherill, G. W. 2001, M&PS, 36, 381
- Chambers, J. E. 2013, Icarus, 224, 43
- Clement, M. S., Kaib, N. A., Raymond, S. N., Chambers, J., E. & Walsh, K. J. 2019a, Icarus, 321, 778
- Clement, M. S., Kaib, N. A. & Chambers, J. E. 2019b, AJ, 157, article id. 208
- Clement, M. S., Chambers, J. E. & Jackson, A. P. 2021a, AJ, 161, id.240
- Clement, M. S. & Chambers, J. E. 2021b, AJ, 162, id.3
- Clement, M. S., Kaib, N. A., Raymond, S. N. & Chambers, J., E. 2021c, Icarus, 367, article id. 114585
- Collins, G. S., Melosh, H. J. & Ivanov, B. A. 2004, M&PS, 39, 217
- Crespi, S., Dobbs-Dixon, I., Georgakarakos, N., Haghighipour, N., Maindl, T. I., Schäfer, C. M. & Winter, P. M. 2021, MNRAS 508, 6013
- Darriba, L. A. & Haghighipour, N. 2021, ApJ (submitted)
- Genda, H., Kokubo, E. & Ida, S. 2012, ApJ, 744, 137
- Genda, H., Kobayashi, H. & Kokubo, E. 2015, ApJ, 810, 136
- Grady, D. E. & Kipp, M. E. 1980, Int. J. Rock Mech. Min. Sci. Geomech. Abstr., 17, 147
- Haghighipour, N. & Winter O. C. 2016, CeMDA, 124, 235
- Ida, S. & Makino, J., 1992, Icarus, 98, 28
- Izidoro, A., Torres, K. S., Winter, O. C. & Haghighipour, N. 2013, ApJ, 767, 54
- Izidoro, A., Haghighipour, N., Winter, O. C. & Tsuchida, M. 2014, ApJ 782, 31
- Jutzi, M. 2015, P&SS, 107, 3
- Kobayashi, H. & Tanaka, H. 2010, Icarus, 206, 735
- Kokubo, E. & Ida, S. 1998, Icarus, 131, 171

- Kokubo, E. & Ida, S. 2010, *Icarus*, 143, 15
- Kokubo, E., Kominami, J. & Ida, S. 2006, *ApJ*, 642, 1131
- Kokubo, E. & Genda, H. 2010, *ApJL*, 714L, 21
- Lange, M. A., Ahrens, T. J. & Boslough, M. B. 1984, *Icar*, 58, 383
- Leinhardt, Z. M. & Stewart, S. T. 2012, *ApJ*, 745, 79
- Levison, H. F. & Agnor C. 2003, *AJ*, 125, 2692
- Maindl, T. I., Schäfer, C., Speith, R., Süli, Á., Forgács-Dajka, E. & Dvorak, R. 2013, *Astron. Nachr.*, 334, 996
- Maindl, T. I., Dvorak, R., Schäfer, C. & Speith, R. 2014, in: *Complex Planetary Systems, Proceedings of the International Astronomical Union Symposium*, 310, 138
- Marcus, R. A., Stewart, S. T., Sasselov, D. & Hernquist, L., 2009, *ApJL*, 700, L118
- Marcus, R. A., Sasselov, D., Stewart, S. T. & Hernquist, L. 2010, *ApJL*, 719, L45
- Melosh, H. J. 1996, *Impact Cratering* (Oxford: Oxford Univ. Press)
- Melosh, H. J. & Ryan, E. V. 1997, *Icar*, 129, 562
- Michel, P. 2009, *Lect. Notes Phys.*, 758, 99
- Monaghan, J. J. & Gingold, R. A. 1983, *J. Comput. Phys.*, 52, 374
- Morbidelli, A., Chambers, J., Lunine, J. I., Petit, J. M., Robert, F., Valsecchi, G. B. & Cyr, K. E. 2000, *M&PS*, 35, 1309
- Morishima, R., Schmidt, M. W., Stadel, J. & Moore, B. 2008, *ApJ*, 685, 1247
- Nakamura, A. M., Michel, P., & Setoh, M. 2007, *JGRE*, 112, E02001
- Nakamura, A. M. & Michel, P. 2009, *Lect. Notes Phys.*, 758, 71
- Nesvorny, D., Roig, F. V. & Deienno R. 2021, *AJ*, 161, 50
- O’Brien, D. P., Morbidelli, A. & Levison, H. F. 2006, *Icarus*, 184, 39
- O’Brien, D. P., Walsh, K. J., Morbidelli, A., Raymond, S. N. & Mandell, A. M. 2014, *Icarus*, 239, 74

- O’Brien, D. P., Izidoro, A., Jacobson, S. A., Raymond, S. N., & Rubie, D. C. 2018, *Space Sci. Rev.*, 214, 47
- Raymond, S. N., Quinn, T. & Lunine, J. I. 2005a, *Icarus*, 177, 256
- Raymond, S. N., Quinn, T. & Lunine, J. I. 2005b, *ApJ*, 632, 670
- Raymond, S. N., O’Brien, D. P., Morbidelli, A. & Kaib, N. A. 2009, *Icarus*, 203, 644
- Schäfer, C., Speith, R. & Kley, W. 2007, *A&A*, 470, 733
- Schäfer, C., Riecker, S., Maindl, T. I., Scherrer, S., Speith, R. & Kley, W. 2016, *A&A*, 590, A19
- Schäfer, C. M., Wandel, O. J., Burger, C., et al. 2020, *Astron. Comput.*, 33, 100410
- Stewart, S. T. & Leinhardt, Z. M. 2012, *ApJ*, 751, 32
- Tillotson, J. H. 1962, *Metallic Equations of State for Hyper-velocity Impact*, General Atomic Rep. GA-3216 (San Diego, CA: General Atomic)
- Wallace J., Tremaine, S. & Chambers, J. 2017, *AJ*, 154, 175
- Walsh, K. J., Morbidelli, A., Raymond, S. N., O’Brien, D. P. & Mandell, A. M. 2011, *Nature*, 475, 206
- Weibull, W. A. 1939, *Ingvetensk. Akad. Handl.*, 151, 5

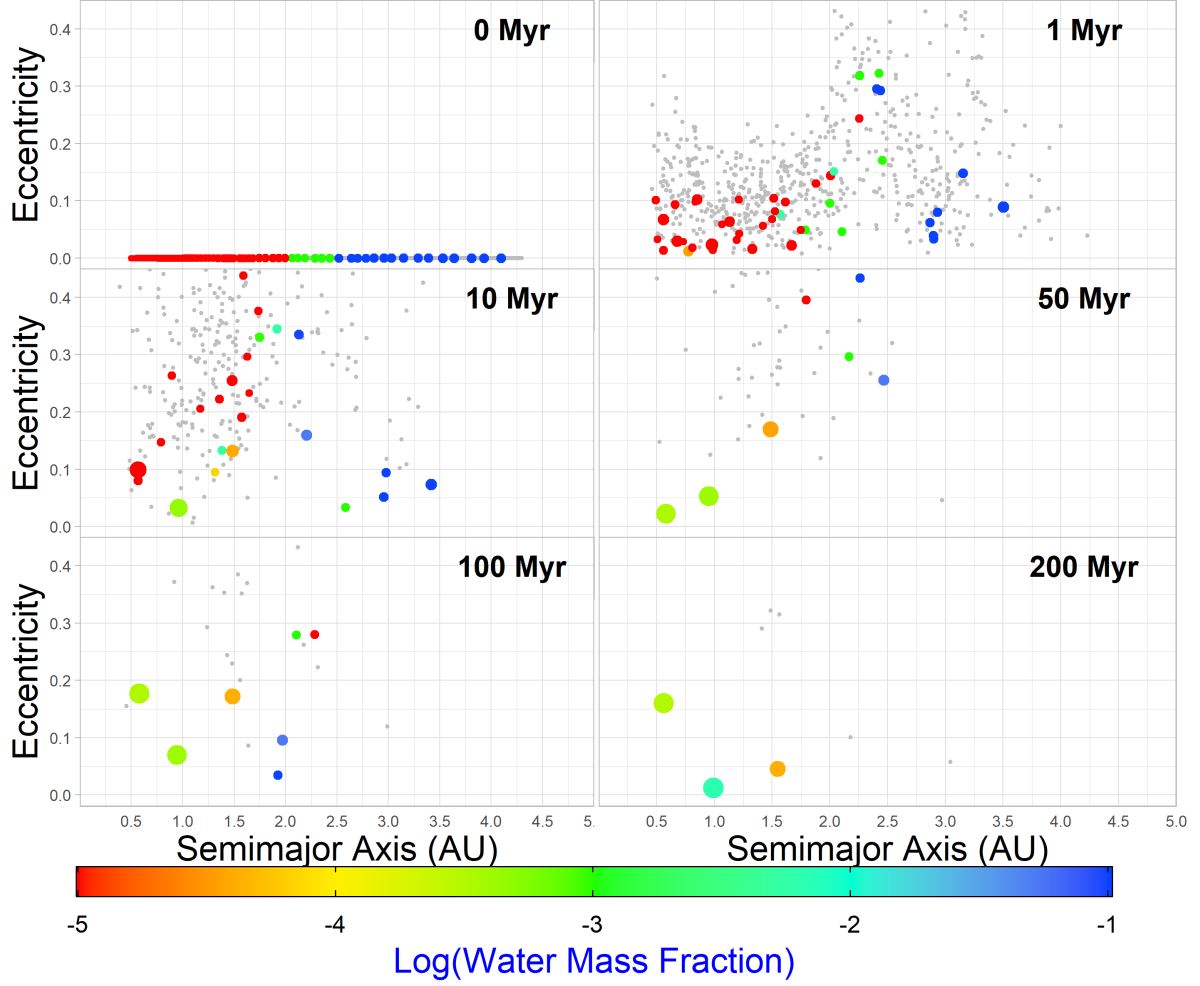


Fig. 1.— Sample of the simulations of terrestrial planet formation in the classical model. In this simulation, Jupiter and Saturn are in their current orbits and carry their current eccentricities. Planetary embryos are color coded based on their water-content. Planetesimals are shown by color gray in the background. The masses of the embryos are proportional to their radii.

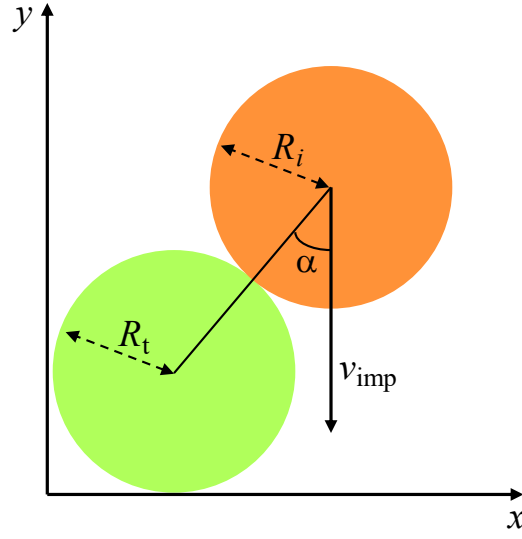


Fig. 2.— Geometry of an impact. The target in light green is at rest. The impactor is in orange. The quantities v_{imp} and α are the impact velocity and impact angle, respectively.

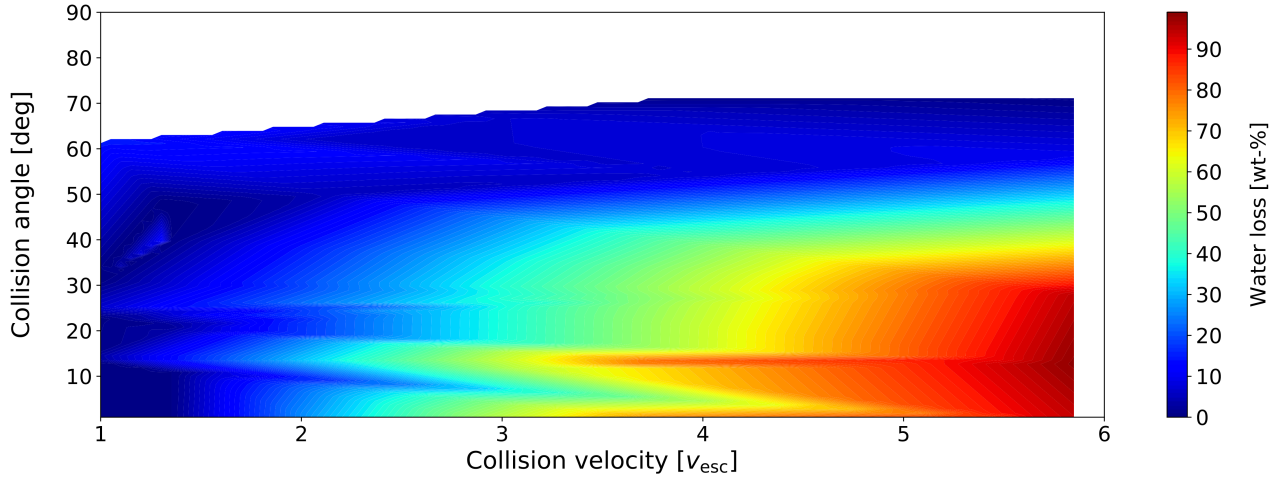


Fig. 3.— SPH simulation of water-loss in the collision of two Ceres-mass objects. The target is silicate rock (basalt) with 30% water-mass fraction. The projectile is 100% basaltic rock. The color-coding represents the amount of water lost in one collision in terms of the initial water-mass. For instance, color yellow indicates that 60% of the total water that initially existed before the impact was lost in the form of debris. See figure 2 for the geometry of an impact.

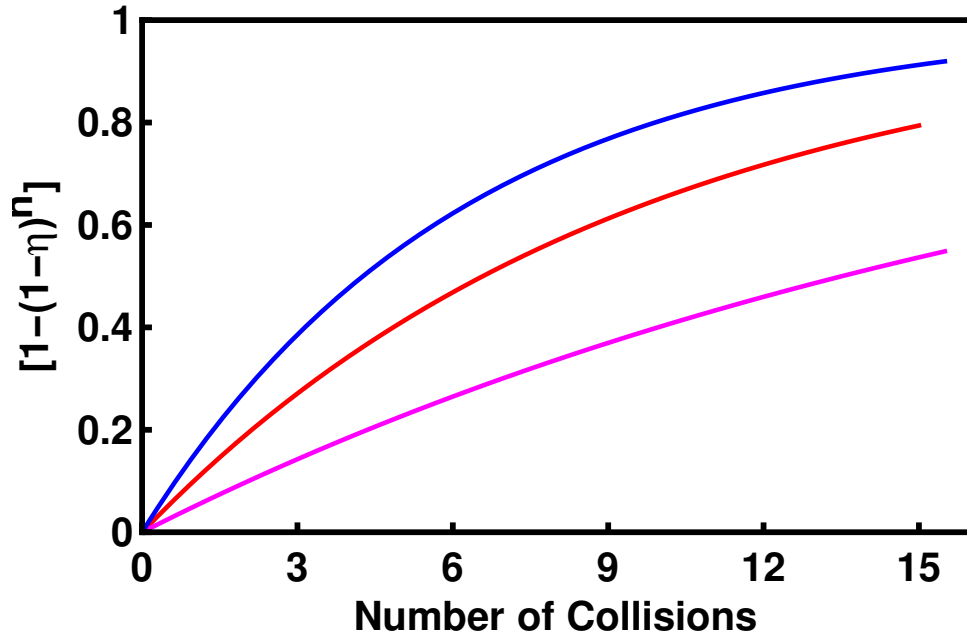


Fig. 4.— Graph of the quantity $[1 - (1 - \eta)^n]$ in equation (2) for different number of impacts (n) and for the values of $\eta = 5\%$ (Cyan), 10% (red) and 15% (blue). The figure shows the fraction of the mass that is lost from the first target after n collisions. As shown here, after a few impacts, the loss of mass is not negligible.

Table 1. Material parameters for basalt and ice.

Parameters	Basalt	Ice	Reference
Bulk density ρ_0 [kg/m ³]	2700	917	(Melosh 1996)
A_T (Tillotson EOS parameter) [GPa]	26.7	9.47	(Melosh 1996)
B_T (Tillotson EOS parameter) [GPa]	26.7	9.47	(Melosh 1996)
E_0 (Tillotson EOS parameter) [MJ/kg]	487	10	(Melosh 1996)
E_{iv} (Tillotson EOS parameter) [MJ/kg]	4.72	0.773	(Melosh 1996)
E_{cv} (Tillotson EOS parameter) [MJ/kg]	18.2	3.04	(Melosh 1996)
a_T (Tillotson EOS parameter)	0.5	0.3	(Melosh 1996)
b_T (Tillotson EOS parameter)	1.5	0.1	(Melosh 1996)
α_T (Tillotson EOS parameter)	5	10	(Melosh 1996)
β_T (Tillotson EOS parameter)	5	5	(Melosh 1996)
K (Bulk modlus) [GPa]	36.7	9.47	(Benz & Asphaug 1999)
μ (Shear modulus) [GPa]	22.7	2.8	(Benz & Asphaug 1999)
Y_0 (Yield stress) [GPa]	3.5	1	(Benz & Asphaug 1999)

Table 2. Post-collision mass and water-content of the final planets in figure 1

	Planet-1	Planet-2	Planet-3
Seed embryo	Embryo-8	Embryo-28	Embryo-30
Initial mass [Mars-mass]	0.15	0.23	0.24
Initial semimajor axis [AU]	0.59	0.99	1.04
Initial WMF [%]	0.001	0.001	0.001
Final semimajor axis [AU]	0.56	0.99	1.55
Final eccentricity	0.16	0.01	0.04
Collisions with embryos	10	10	7
Collisions with planetesimals	79	44	18
Total embryo-embryo collisions	18	18	9
Total embryo-planetesimal collisions	171	125	42
Total mass-loss [Mars-mass]	2.52	3.46	1.10
Final mass [Mars-mass]	4.53	4.67	2.27
Perfect-Merging mass [Mars-mass]	7.31	8.18	3.17
Error in mass [%]	38	43	29
Final WMF [%]	0.08	0.18	
Perfect-Merging WMF [%]	0.10	0.22	
Error in WMF [%]	16	18.3	